Zhou et al. *Zool. Res.* 2025, 46(3): 722−732
https://doi.org/10.24272/j.issn.2095-8137.2024.378
https://cstr.cn/32248.14.zr.2024.378

ZR | Zoological Research

Article Open Access

HNRNPA2B1-mediated m6A modification enhances lncRNA NORHA stability to control granulosa cell functions

Chun-Xue Zhou[1], Si-Qi Wang[1], Ji-Yu Zhang[1], Xing Du[1], Qi-Fa Li[1,*]

[1] *College of Animal Science and Technology*, *Nanjing Agricultural University*, *Nanjing*, *Jiangsu* 210095, *China*

ABSTRACT

NORHA, a long non-coding RNA (lncRNA), serves as a key inducer of follicular atresia in sows by triggering granulosa cells (GCs) apoptosis. However, its regulation by N6-methyladenosine (m6A)—the most abundant RNA modification—remains unresolved. This study identified NORHA as a functional target of the m6A reader HNRNPA2B1 in sow GCs (sGCs). Transcriptome-wide mapping of RNA modification sites revealed extensive m6A enrichment on NORHA, with HNRNPA2B1 binding directly to the transcript and enhancing its stability via modification of multiple m6A sites, including A261, A441, and A919. HNRNPA2B1 suppressed 17β-estradiol (E2) biosynthesis and promoted sGC apoptosis by activating the NORHA-FoxO1 axis. FoxO1 subsequently repressed expression of cytochrome P450 family 19 subfamily A member 1 (CYP19A1), which encodes the enzyme essential for E2 biosynthesis. Additionally, HNRNPA2B1 functioned as a critical mediator of METTL3-dependent m6A modification, modulating NORHA expression and activity in sGCs. This study highlights an important m6A-dependent regulatory mechanism governing NORHA expression in sGCs.

Keywords: LncRNA NORHA; m6A modification; HNRNPA2B1; FoxO1; Sow granulosa cells

INTRODUCTION

RNA modifications introduce chemical diversity to transcripts without altering their nucleotide sequences, establishing an epitranscriptomic regulatory layer that modulates post-transcriptional expression of genes. To date, nearly 170 distinct RNA modifications have been identified across diverse cell types, influencing the structure and function of various RNA species, including messenger RNAs (mRNAs) and non-coding RNAs (ncRNAs) (Wiener & Schwartz, 2021; Zhao et al., 2023). Among these, modifications such as methylation (e.g., N1-methyladenosine (m1A), 5-methylcytidine (m5C), N6-methyladenosine (m6A), and N7-methylguanosine (m7G)), phosphorylation (e.g., 2'-uridine phosphate (UP)), and acetylation (e.g., N4-acetylcystidine (ac4C)) have been most extensively characterized in eukaryotes (Cai et al., 2024; Chen et al., 2024; Zhao et al., 2023). These RNA modifications are indispensable for embryogenesis and cell cycle regulation, while their dysregulation has been implicated in embryonic lethality, congenital abnormalities, and a broad spectrum of diseases (Sun et al., 2023a; Yang et al., 2024b).

Among internal RNA modifications, m6A is the most abundant and functionally versatile. Notably, m6A is dynamic and reversible, and plays essential roles in a range of physiological processes, including stress responses and embryonic development, by regulating RNA transcription, splicing, localization, translation, and degradation (Yang et al., 2024a). Methyltransferase complexes (writers), such as methyltransferase-like 3 (METTL3), WT1-associated protein (WTAP), and methyltransferase-like 14 (METTL14), catalyze the methylation of adenosine (A) in RNA, while demethylases (erasers) such as fat mass and obesity-associated protein (FTO) and AlkB homolog 5 (ALKHB5) catalyze the demethylation of m6A modification sites (Garbo et al., 2024; Zaccara et al., 2019). The functional consequences of m6A are mediated via recognition by specific reader proteins, such as members of the YTH and IGFBP families, and heterogeneous nuclear ribonucleoprotein A2B1 (HNRNPA2B1) (Wiener & Schwartz, 2021; Yang et al., 2024b). HNRNPA2B1, a powerful m6A reader of the HNRNP family, recognizes and interacts with m6A-harboring primary miRNAs (pri-miRNAs) and precursor mRNAs (pre-mRNAs) to control miRNA biogenesis and mRNA stability (Alarcón et al., 2015; Yu et al., 2024). However, its role in regulating long ncRNAs (lncRNAs) remains largely unknown.

NORHA (noncoding RNA highly expressed in atretic follicles) is a cytoplasmic lncRNA that promotes apoptosis in sow granulosa cells (sGCs), thereby contributing to follicular atresia. It exerts its effects via modulation of the miR-183-96-182 cluster and activation of forkhead box O1 (FoxO1) signaling (Yao et al., 2021). As the most strongly up-regulated

Received: 22 January 2025; Accepted: 17 February 2025; Online: 18 February 2025

Foundation items: This work was supported by the National Natural Science Foundation of China (32072693), Fundamental Research Funds for the Central Universities (KYLH2025010), and Postgraduate Research & Practice Innovation Program of Jiangsu Province（KYCX24-0994）

*Corresponding author, E-mail: liqifa@njau.edu.cn

lncRNA during sow follicular atresia, NORHA has attracted attention as a potential regulatory node in reproductive biology (Li et al., 2023; Wang et al., 2023a; Yang et al., 2023b). Transcriptional repression of NORHA in sGCs has been attributed to MEIS1, a TALE-family transcription factor that binds its core promoter (Wang et al., 2023b), whereas miR-23a has been shown to activate its transcription by acting as a small activating RNA (saRNA) (Wang et al., 2022). Nonetheless, mechanisms regulating NORHA at the post-transcriptional level remain unclear. This study demonstrated that the m6A reader HNRNPA2B1 facilitates the stability of the NORHA transcript in sGCs by promoting m6A methylation at specific adenosine residues. This m6A-dependent stabilization of NORHA suppresses 17β-estradiol (E2) biosynthesis in sGCs, providing new mechanistic insight into the post-transcriptional control of follicular atresia.

MATERIALS AND METHODS

Bioinformatics

NORHA and cytochrome P450 family 19 subfamily A member 1 (CYP19A1) PII promoter sequences of pigs were obtained from our previous studies (Li et al., 2018; Yao et al., 2021). RNA secondary structure prediction for the NORHA transcript was performed using RNAfold (http://rna.tbi.univie.ac.at/cgi-bin/RNAWebSuite/RNAfold.cgi). Candidate RNA-binding proteins (RBPs) predicted to interact with NORHA were identified using catRAPID (http://s.tartaglialab.com/page/catrapid_group) and RBPSuite (http://www.csbio.sjtu.edu.cn/bioinf/RBPsuite/). Gene Ontology (GO) enrichment analysis was conducted using DAVID (https://david.ncifcrf.gov/). Putative RNA modification sites within the NORHA transcript were predicted using multiple online tools (Supplementary Table S1). The tertiary structure of the HNRNPA2B1 protein was modeled with SWISS-MODEL (https://swissmodel.expasy. org). FoxO1 response elements (FREs) in the CYP19A1 PII promoter were searched using JASPAR 2024 (https://jaspar.elixir.no/).

Follicle collection

Antral follicles (3–5 mm in diameter) were isolated from freshly harvested ovaries of commercial sows (*n*=200) (Zhushun, China). Follicular fluid was extracted using a syringe, and the remaining tissue was centrifuged to extract total RNA and protein. The cell pellet was used to isolate sGCs, and the supernatant was reserved for quantification of progesterone (P4) and E2 levels using a P4 and E2 Radioimmunoassay Kit (North Pharmaceutical, China). Follicles were classified as healthy or atretic based on the P4:E2 ratio, a well-known indicator of follicular atresia.

sGCs culture

sGCs were washed with phosphate-buffered saline (PBS), resuspended, seeded in culture plates, and cultured in an incubator at 37°C and 5% CO_2 in Dulbecco's Modified Eagle Medium/Nutrient Mixture F-12 (DMEM/F12, Gibco, USA) containing 10% fetal bovine serum (FBS) (Gibco, USA).

RNA immunoprecipitation (RIP)-qPCR

RIP-qPCR was carried out using protein A/G magnetic beads (Selleck, China) following the manufacturer's instructions. Briefly, 5 μg of specific antibody (Supplementary Table S2) was incubated with the beads for 1 h at room temperature, followed by six washes. The antibody-conjugated beads were then incubated with cell lysates in RIP buffer. Immunoprecipitated RNA was extracted using TRIzol reagent (Accurate Biology, China) and purified for qPCR with specific primers (Supplementary Table S3). Total RNA served as the input control.

Plasmids and small interfering RNAs (siRNAs)

The pcDNA3.1-basic vector was obtained from Promega (Madison, USA). Full-length coding sequences of HNRNPA2B1 and METTL3 were amplified from sGCs and inserted into the vector to generate overexpression constructs. Primer sequences are shown in Supplementary Table S4. Overexpression constructs for NORHA and FoxO1 were prepared previously (Yao et al., 2021). Reporter constructs of the PII promoter were prepared by Tsingke (China). All siRNAs were synthesized by GenePharma (China) and are listed in Supplementary Table S5.

qPCR

qPCR was conducted as previously described (Wang et al., 2023b), with AceQ qPCR SYBR Green Master Mix (Vazyme, China) and specific primers (Supplementary Table S6).

Western blot analysis

Western blot analysis was conducted using the protocols, instruments, and software described in our previous study (Wang et al., 2023b), with GAPDH used as the internal reference. All antibodies are provided in Supplementary Table S2.

RNA stability

After treatment with actinomycin D (ActD) (Aladdin, China) for 0, 1, 2, 3, and 4 h, sGCs were collected for total RNA extraction and qPCR quantification. NORHA transcription levels were normalized by GAPDH, and the half-life ($t_{1/2}$) was calculated.

Immunohistochemistry (IHC)

Sow ovary tissues were fixed with 4% paraformaldehyde and sent to Pinuofei (China) for IHC assay with anti-HNRNPA2B1 antibodies (Supplementary Table S2). Images were acquired using a Nikon Eclipse 80i microscope (Japan).

Apoptosis rate assay

Apoptotic rates were evaluated using an Annexin V-FITC/PI Apoptosis Detection Kit (Vazyme, China) according to the manufacturer's instructions. Samples were analyzed by flow cytometry (Becton Dickinson, USA).

Luciferase assay

Cell lysates were obtained 48 h post-transfection and analyzed using the Duo-Lite Luciferase Assay System (Vazyme, China). Relative luciferase activity (RLU) was calculated by dividing firefly luciferase activity by *Renilla* luciferase activity.

Chromatin immunoprecipitation (ChIP)-PCR

ChIP-PCR was performed following the steps outlined in our recent study (Wang et al., 2023b). Briefly, chromatin from sGCs was immunoprecipitated with an anti-FoxO1 antibody (Supplementary Table S2). Enriched DNA was amplified by PCR using specific primers (Supplementary Table S7) and visualized on agarose gels (Saipu, China).

Statistical analysis and data visualization

Statistical significance was established using Student's *t*-test or one-way analysis of variance (ANOVA). Graphs were

plotted with GraphPad Prism v.9.5 (GraphPad, USA), with each data point representing a biological replicate.

RESULTS

NORHA is modulated by multiple RNA modifications in sGCs

NORHA is an intergenic lncRNA bearing a polyA tail (Yao et al., 2021). Results showed that its primary structure consisted of 456 A, 385 uracil (U), 369 guanine (G), and 385 cytosine (C), with base A having the highest content (28.59%, 456/1 595) (Supplementary Figure S1). Secondary structure prediction using RNAfold revealed 13 asymmetric internal loops, five single-nucleotide bulges, and several unpaired bases forming convex loops that distort the radial architecture and may influence the tertiary structure of RNAs (Figure 1A). In total, 217 RBPs were predicted to interact with the NORHA transcript (Supplementary Table S8). These RBPs were markedly enriched in 200 GO terms related to RNA metabolism, including N6-methyladenosine binding, RNA stability regulation, and miRNA-mediated regulation (Figure 1B). Notably, several of these RBPs were linked to RNA modification, such as m6A reader HNRNPA2B1, m5C methyltransferase NSUN2, and internal m7G reader QKI (Supplementary Table S9), indicating that NORHA may undergo combinatorial post-transcriptional regulation by multiple RNA modifications.

To further examine this possibility, predicted modification sites within the NORHA transcript were identified, revealing 11 putative sites, including five m6A sites, two m7G sites, two m5C sites, one Nm site, and one ac4C site (Figure 1A). Consistent with these findings, multiple RNA modification-related proteins predicted to interact with NORHA were expressed in sow ovaries, including HNRNPA2B1, WTAP, and FBL (Figure 1C). Methylated RIP (MeRIP)-qPCR confirmed m6A enrichment on NORHA in sGCs (Figure 1D). Together, these results demonstrate that NORHA is extensively modified by multiple RNA modifications in sGCs.

HNRNPA2B1 facilitates RNA stability and m6A modification of NORHA

HNRNPA2B1, an established m6A reader, was previously identified as a putative NORHA-binding RBP (unpublished). RIP analysis using anti-HNRNPA2B1 antibodies confirmed that HNRNPA2B1 physically interacted with NORHA in sGCs (Figure 2A). To determine whether HNRNPA2B1 regulates NORHA expression in sGCs, its ectopic expression resulted in a significant up-regulation of NORHA levels (Figure 2B; Supplementary Figure S2). In contrast, silencing HNRNPA2B1

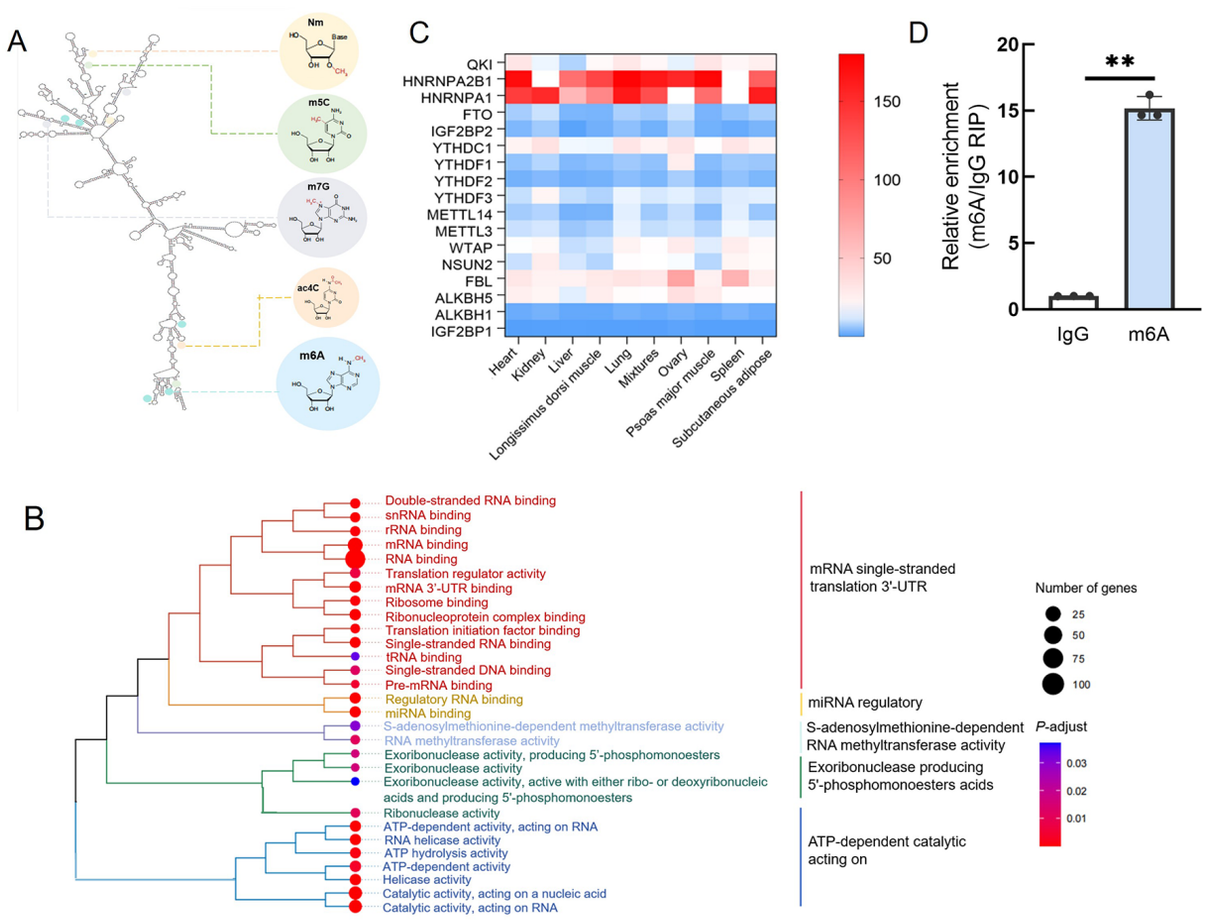

Figure 1 RNA modifications of NORHA in sGCs

A: NORHA RNA structures predicted using RNAfold. Colored circles indicate RNA modifications, with their size indicating number of sites potentially controlled by RNA modifications. B: GO analysis of RBPs potentially interacting with NORHA. GO terms are indicated by various node colors, with their size indicating their significance. C: Electronic tissue expression profile of coding genes for RNA modification-related proteins predicted to interact with NORHA in pigs. D: MeRIP-qPCR was employed to determine m6A-modified NORHA RNAs immunoprecipitated with anti-m6A antibody in sGCs. Values are mean±standard error. **: P<0.01.

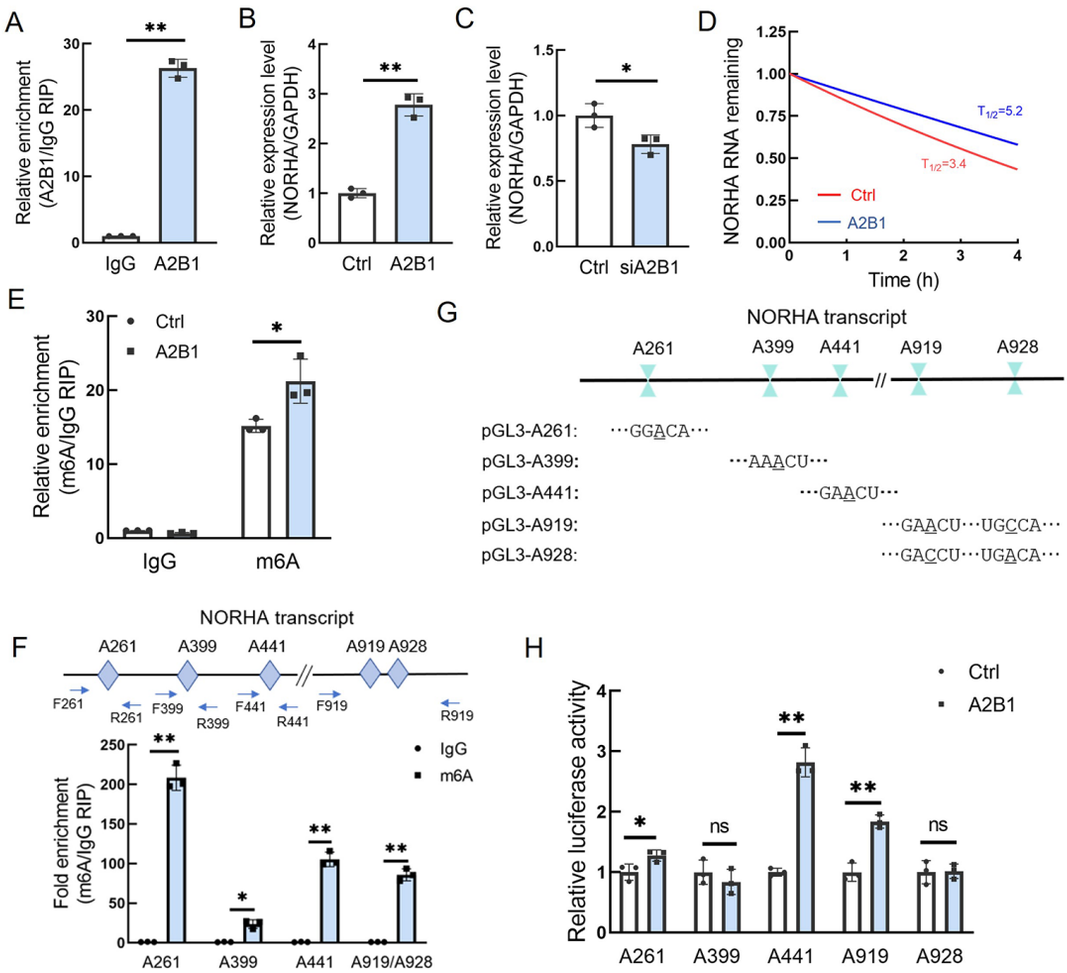

Figure 2 HNRNPA2B1 promotes RNA stability and m6A modification of NORHA in sGCs

A: RIP assay. NORHA enrichment was detected using an anti-HNRNPA2B1 antibody. qPCR was used to quantify immunoprecipitated RNAs. HNRNPA2B1 is abbreviated as A2B1. B, C: NORHA expression levels in sGCs following ectopic expression (B) or silencing (C) of HNRNPA2B1. D: RNA stability assay. After transfection of pcDNA3.1-HNRNPA2B1 for 10 h, cells were treated with actinomycin D (ActD) and collected at 0, 1, 2, 3, and 4 h to quantify NORHA expression. E: MeRIP-qPCR assay. qPCR was employed to determine m6A-containing NORHA RNAs from sGCs immunoprecipitated with anti-m6A antibody. F: MeRIP-qPCR assay. Specific primers (top) designed to amplify m6A-modified regions of NORHA, and qPCR results of immunoprecipitated RNA (bottom). G, H: Luciferase assays. Reporter vectors of NORHA transcript harboring m6A sites were constructed (G) and co-transfected with pcDNA3.1-HNRNPA2B1 into sGCs, and luciferase activities were determined (H). Values are mean±standard error. *: P<0.05; **: P<0.01; ns: Not significant.

resulted in a marked decrease in NORHA abundance (Figure 2C; Supplementary Figure S3), indicating that HNRNPA2B1 positively regulates NORHA in sGCs.

HNRNPA2B1 is known to stabilize its target RNAs by preventing degradation (Jin et al., 2024). Consistent with this role, HNRNPA2B1 overexpression prolonged NORHA stability, increasing its half-life from 3.4 h to 5.2 h (Figure 2D). To determine whether this stabilization involves m6A methylation, MeRIP-qPCR revealed increased m6A enrichment on the NORHA transcript following HNRNPA2B1 overexpression (Figure 2E), indicating that HNRNPA2B1 enhances NORHA stability through m6A modification. Among the five putative m6A sites, methylation was significantly elevated at A261, A399, A441, and A919 in response to HNRNPA2B1 overexpression (Figure 2F), consistent with computational prediction. These findings were further validated by luciferase reporter assays (Figure 2G–H). Collectively, these findings demonstrate that HNRNPA2B1 enhances RNA stability of NORHA in sGCs by promoting its m6A modification.

HNRNPA2B1 induces sGC apoptosis via NORHA

A 1 026 bp coding sequence (CDS) of HNRNPA2B1 was isolated from sGCs. HNRNPA2B1 was located on *Sus scrofa* chromosome 18 and exhibited high nucleotide conservation with its human and mouse orthologs, sharing 95.71% and 92.88% identities, respectively (Supplementary Figure S4). The porcine HNRNPA2B1 polypeptide was composed of 341 amino acids and was highly conserved relative to that of humans and mice, with 100% and 99.71% identities, respectively (Supplementary Figure S5A). Importantly, similar to that of humans and mice, the porcine HNRNPA2B1 protein contained multiple classical domains, including an RNA-recognition motif (RRM) (aa 10–173), ELAV_HUD_SF (aa 102–149), and PABP-1234 (aa 6–148) (Supplementary Figure S5A). Tertiary structure modeling predicted a fold composed of four α-helices and eight β-folds (Supplementary Figure S5B), supporting functional conservation across species.

Transcriptomic data showed widespread expression of HNRNPA2B1 in various tissues, with notable abundance in the sow ovary (Figure 3A). IHC assay results revealed low

HNRNPA2B1 protein expression in healthy follicles from the primordial to mature stage (Figure 3B), but markedly elevated expression in sGCs from atretic follicles (Figure 3B). Western blotting confirmed a significant increase in HNRNPA2B1 protein levels in atretic follicles (Figure 3C; Supplementary Figure S6), implicating HNRNPA2B1 in the regulation of follicular atresia. To further explore its functional role, HNRNPA2B1 was overexpressed in sGCs, resulting in a significant increase in apoptotic cell populations (Figure 3D; Supplementary Figure S7), indicating that HNRNPA2B1 acts as a pro-apoptotic m6A reader. Notably, knockdown of NORHA attenuated HNRNPA2B1-induced apoptosis (Figure 3D; Supplementary Figure S7) and restored the decreased BCL2/BAX ratio (Figure 3E), suggesting that HNRNPA2B1 promotes apoptosis via NORHA. Furthermore, HNRNPA2B1 also enhanced the translation of FoxO1, a downstream effector of NORHA implicated in oxidative stress in sGCs (Sheng et al., 2024; Yao et al., 2021), while NORHA knockdown reversed this effect (Figure 3F). Collectively, these findings identify HNRNPA2B1 as a conserved pro-apoptotic m6A reader that induces apoptosis in sGCs by enhancing NORHA expression and activating the downstream FoxO1 signaling axis.

HNRNPA2B1 suppresses E2 biosynthesis via NORHA

To investigate the relationship between HNRNPA2B1 and sow follicular atresia *in vivo*, levels of P4 and E2 were measured in follicular fluid, and the P4:E2 ratio was calculated. A significant positive correlation was observed between the P4:E2 ratio and follicular HNRNPA2B1 expression (Figure 4A), reinforcing its association with atresia progression. Conversely, HNRNPA2B1 expression was negatively correlated with E2 concentrations in follicular fluid (Figure 4B), suggesting that HNRNPA2B1 may influence the steroidogenic function of sGCs. Consistent with this, ectopic expression of HNRNPA2B1 in sGCs resulted in a marked reduction in E2 levels in the culture medium (Figure 4C). This was accompanied by decreased expression of CYP19A1, which encodes the limiting enzyme (P450arom) for E2 biosynthesis (Figure 4D, E). These findings suggest that HNRNPA2B1 represses E2 production by down-regulating CYP19A1.

To determine whether this repression is mediated through NORHA, co-transformation experiments were performed. Results showed that NORHA knockdown reversed the HNRNPA2B1-induced decline in E2 and CYP19A1 levels in sGCs (Figure 4C–E). Furthermore, overexpression of NORHA alone was sufficient to suppress E2 secretion and reduce CYP19A1 levels in sGCs (Figure 4F–H). Taken together,

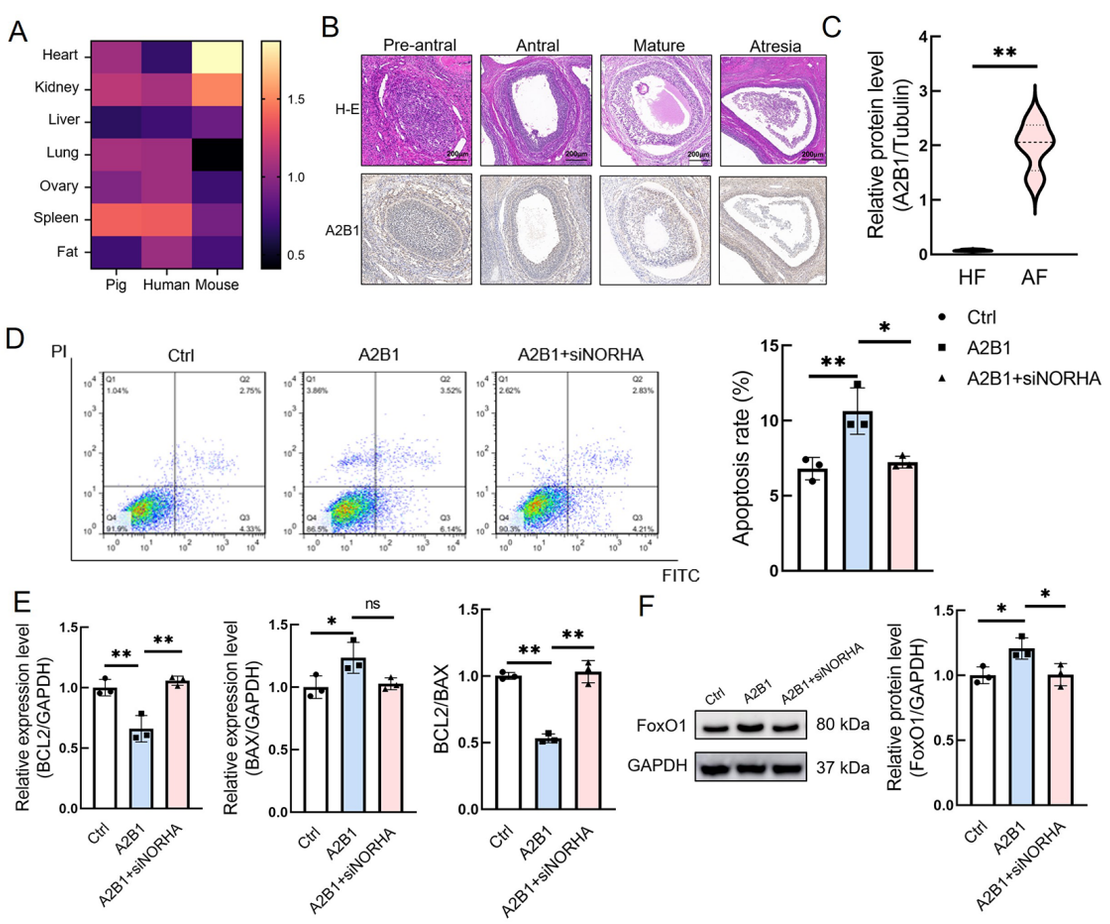

Figure 3 HNRNPA2B1 promotes apoptosis in sGCs via NORHA

A: Cross-species tissue expression profile of HNRNPA2B1 gene in pigs, humans, and mice based on NCBI data. B: Immunohistochemical detection of HNRNPA2B1 in sow ovaries using anti-HNRNPA2B1 antibodies. C: Comparison of HNRNPA2B1 protein levels in healthy and atretic follicles by western blot analysis. Band images are shown in Supplementary Figure S6. HF, healthy follicles. AF, atretic follicles. D–F: sGCs were co-transfected with pcDNA3.1-HNRNPA2B1 and NORHA-siRNA. Apoptosis was assessed by flow cytometry (D). BCL2 and BAX mRNA levels were determined by qPCR, with their ratio then calculated (E). FoxO1 levels were determined using western blotting (F). Values are mean±standard error. *: P<0.05; **: P<0.01; ns: Not significant.

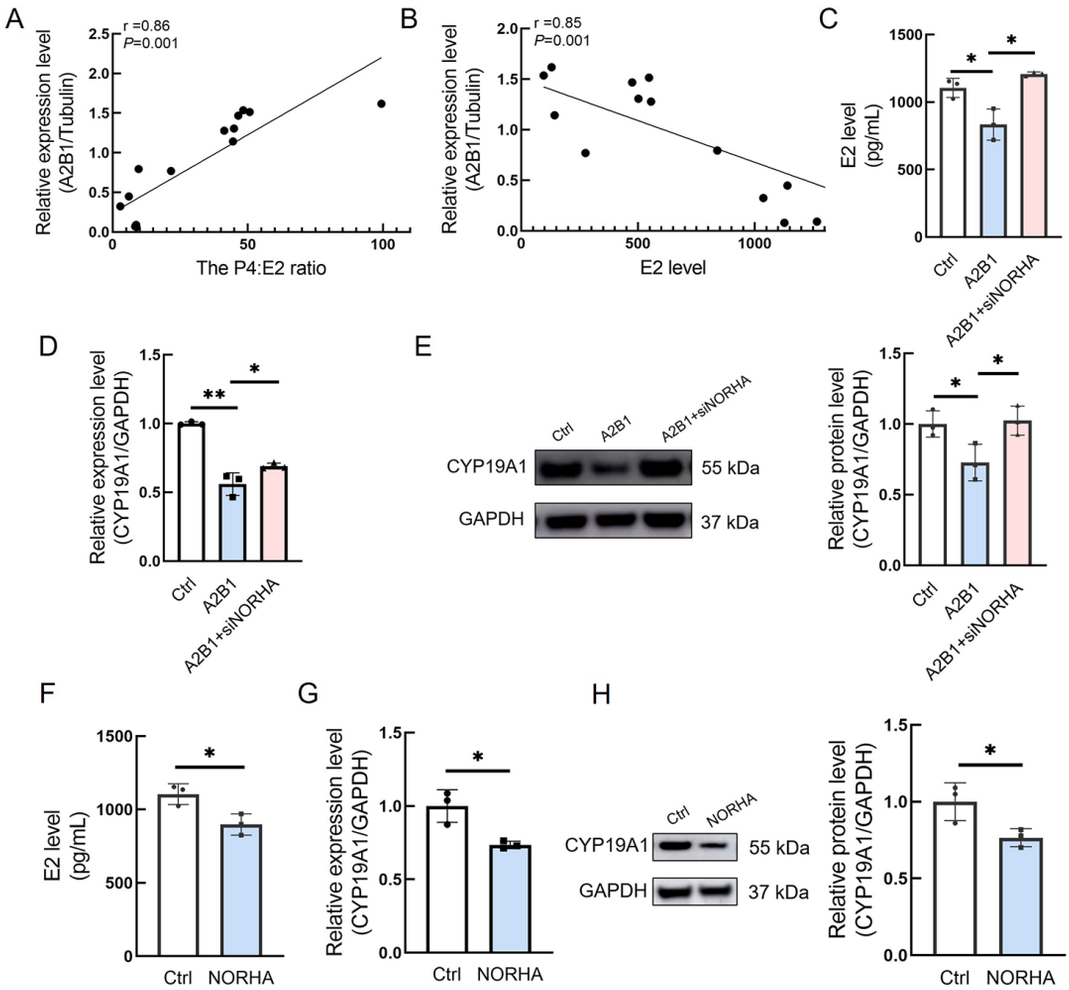

Figure 4 HNRNPA2B1 suppresses E2 biosynthesis in sGCs via NORHA

A, B: Correlation analysis between follicular HNRNPA2B1 expression and the P4:E2 ratio (A) or E2 concentration in follicular fluid (B). C–E: sGCs were co-transfected with pcDNA3.1-HNRNPA2B1 and NORHA-siRNA. E2 concentration in the culture medium was determined by ELISA (C), while CYP19A1 mRNA (D) and protein (E) levels were assessed. F–H: sGCs were transfected with pcDNA3.1-NORHA. E2 concentration (F), CYP19A1 mRNA (G), and protein (H) levels were measured. Values are mean±standard error. *: P<0.05; **: P<0.01.

these results demonstrate that HNRNPA2B1 acts as an m6A reader that inhibits E2 biosynthesis in sGCs via up-regulation of the downstream lncRNA NORHA.

FoxO1 functions as a novel transcriptional suppressor of CYP19A1 in sGCs

During previous characterization of the ovarian-specific PII promoter of the porcine CYP19A1 gene, three putative FREs were identified, including FRE1 (−241/−226 nt), FRE2 (−390/−380 nt), and FRE3 (−747/−735 nt) (Figure 5A; Supplementary Figure S8). To verify the effect of FoxO1 on CYP19A1 activity, three reporter constructs containing individual FRE motifs within the PII promoter were generated (Figure 5B). Luciferase reporter assays revealed a marked reduction in the RLU of PII promoters containing FRE2 and FRE3 (Figure 5C), indicating that FoxO1 restrains CYP19A1 transcriptional activity via these elements. Furthermore, ChIP assays confirmed enrichment of FoxO1 at the FRE2/3 motifs on the PII promoter in sGCs (Figure 5D), demonstrating direct binding of FoxO1 to these regulatory regions.

To assess whether FoxO1 restrains endogenous CYP19A1 expression in sGCs, FoxO1 was ectopically expressed in sGCs, resulting in a marked decline in CYP19A1 (Figure 5E, F; Supplementary Figure S9). Conversely, FoxO1 knockdown led to a pronounced increase in CYP19A1 expression (Figure 5G, H; Supplementary Figure S10), confirming its repressive role. Correspondingly, E2 levels in the culture medium decreased following FoxO1 overexpression and increased upon FoxO1 silencing (Figure 5I, J), indicating functional repression of CYP19A1-mediated E2 biosynthesis. Collectively, these results identify FoxO1 as a novel transcriptional suppressor of CYP19A1 in sGCs.

FoxO1 mediates HNRNPA2B1/NORHA axis suppression of E2 biosynthesis

FoxO1 functions as a vital downstream effector of NORHA in sGCs (Yao et al., 2021). To determine whether NORHA influences E2 biosynthesis, NORHA was silenced in sGCs. This led to a significant increase in E2 concentration in the culture medium (Figure 6A), indicating that NORHA negatively regulates E2 biosynthesis. Consistently, CYP19A1 expression was markedly elevated upon NORHA knockdown (Figure 6B, C). Furthermore, ectopic expression of FoxO1 reversed the increase in both E2 levels and CYP19A1 expression induced by NORHA silencing (Figure 6A–C), demonstrating that FoxO1 mediates the inhibitory effect of NORHA on E2

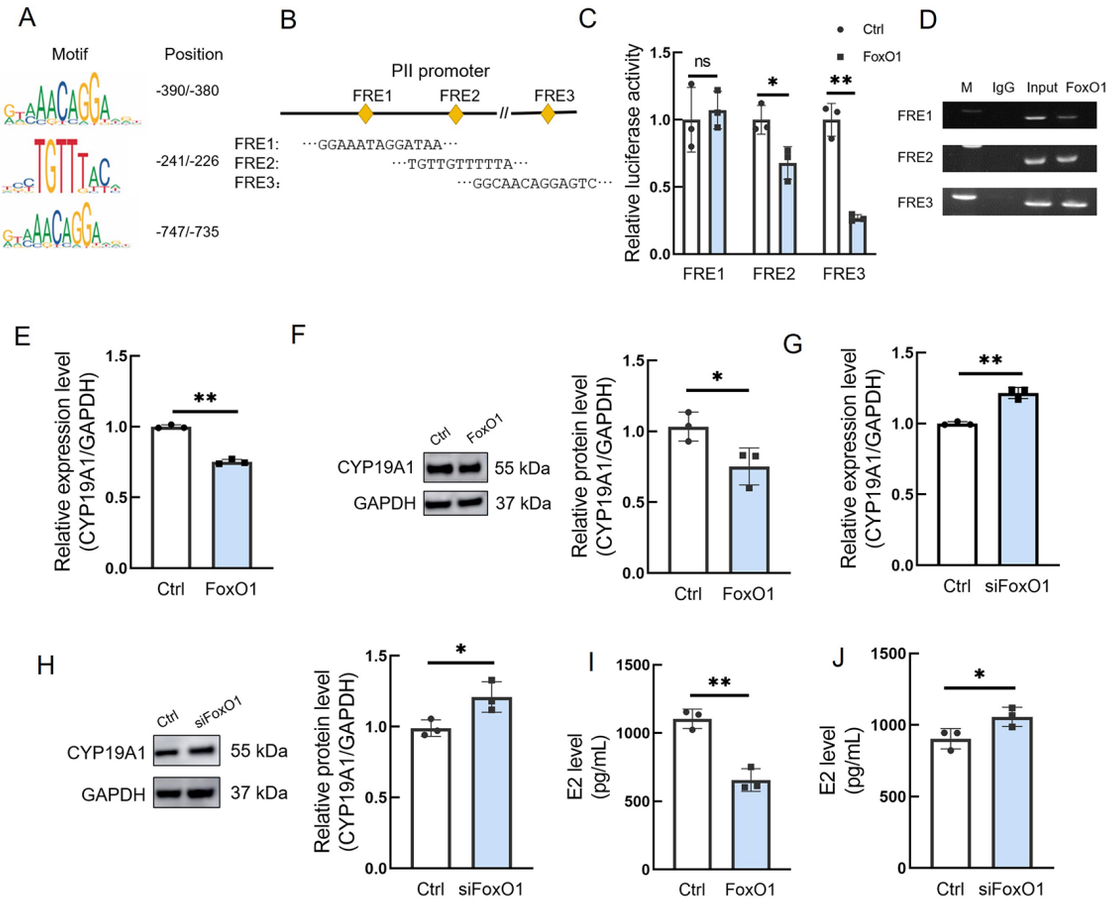

Figure 5 FoxO1 is a novel transcriptional suppressor of CYP19A1 in sGCs

A: Three putative FRE motifs were detected in the PII promoter of the porcine CYP19A1 gene. B: Schematic representation of reporter vectors of the PII promoter. C: Reporter assay. Luciferase activity was measured in sGCs co-transfected with reporter vectors and pcDNA3.1-FoxO1. D: ChIP assay with an anti-FoxO1 antibody was used to determine enrichment of the FoxO1 transcription factor at FRE motifs in the PII promoter. M, marker. E, F: sGCs were transfected with pcDNA3.1-FoxO1, with CYP19A1 mRNA (E) and protein (F) levels then determined. G, H: sGCs were transfected with FoxO1-siRNA, with CYP19A1 mRNA (G) and protein (H) levels then determined. I, J: sGCs were transfected with pcDNA3.1-FoxO1 (I) or FoxO1-siRNA (J), with E2 concentration in the culture medium then determined. Values are mean±standard error. *: $P<0.05$; **: $P<0.01$; ns: Not significant.

biosynthesis.

Our previous results showed that both HNRNPA2B1 and FoxO1 suppress E2 biosynthesis in sGCs (Figure 4C, Figure 5I, J). To test whether FoxO1 functions downstream of HNRNPA2B1 in this regulatory cascade, FoxO1 was silenced in sGCs overexpressing HNRNPA2B1, which restored E2 levels in the culture medium (Figure 6D), confirming that FoxO1 mediates the inhibitory effect of HNRNPA2B1 on E2 biosynthesis in sGCs. Furthermore, FoxO1 knockdown reversed the decline in CYP19A1 induced by HNRNPA2B1 overexpression (Figure 6E, F). Collectively, these findings establish FoxO1 as a central mediator of the HNRNPA2B1/NORHA signaling axis that represses CYP19A1 expression and E2 biosynthesis in sGCs.

HNRNPA2B1 mediates METTL3-dependent regulation m6A modification of NORHA

METTL3, a core methyltransferase, is strongly implicated in HNRNPA2B1 function (Alarcón et al., 2015). To investigate whether METTL3 participates in m6A modification of NORHA in sGCs, MeRIP-qPCR was performed. Ectopic expression of METTL3 resulted in a significant increase in m6A enrichment on NORHA (Figure 7A). Correspondingly, NORHA expression levels were markedly elevated following METTL3 overexpression (Figure 7B), indicating that METTL3 facilitates m6A modification of NORHA in sGCs. However, knockdown of HNRNPA2B1 abolished this increase in NORHA expression (Figure 7B), indicating that HNRNPA2B1 is required for METTL3-mediated regulation. Furthermore, overexpression of METTL3 markedly enhanced the interaction between NORHA and HNRNPA2B1 (Figure 7C). These findings suggest that METTL3 is involved in HNRNPA2B1 induction of NORHA m6A modification in sGCs.

To identify the functional m6A sites through which METTL3 regulates NORHA, luciferase reporter assays were conducted. Results showed a marked increase in the RLU of reporter vectors harboring A261, A441, and A919, but not A399 or A928 in METTL3-overexpressing sGCs (Figure 7D), a pattern consistent with HNRNPA2B1-overexpressing cells. In contrast, METTL3 had no significant effect on reporters carrying mutated versions of A261, A441, or A919 (Figure 7E, F), indicating that METTL3 mediates NORHA via three m6A sites (A261, A441, and A919). Additionally, co-transfection experiments showed that silencing HNRNPA2B1 reversed the METTL3-induced increase in the RLU from wild-type A261,

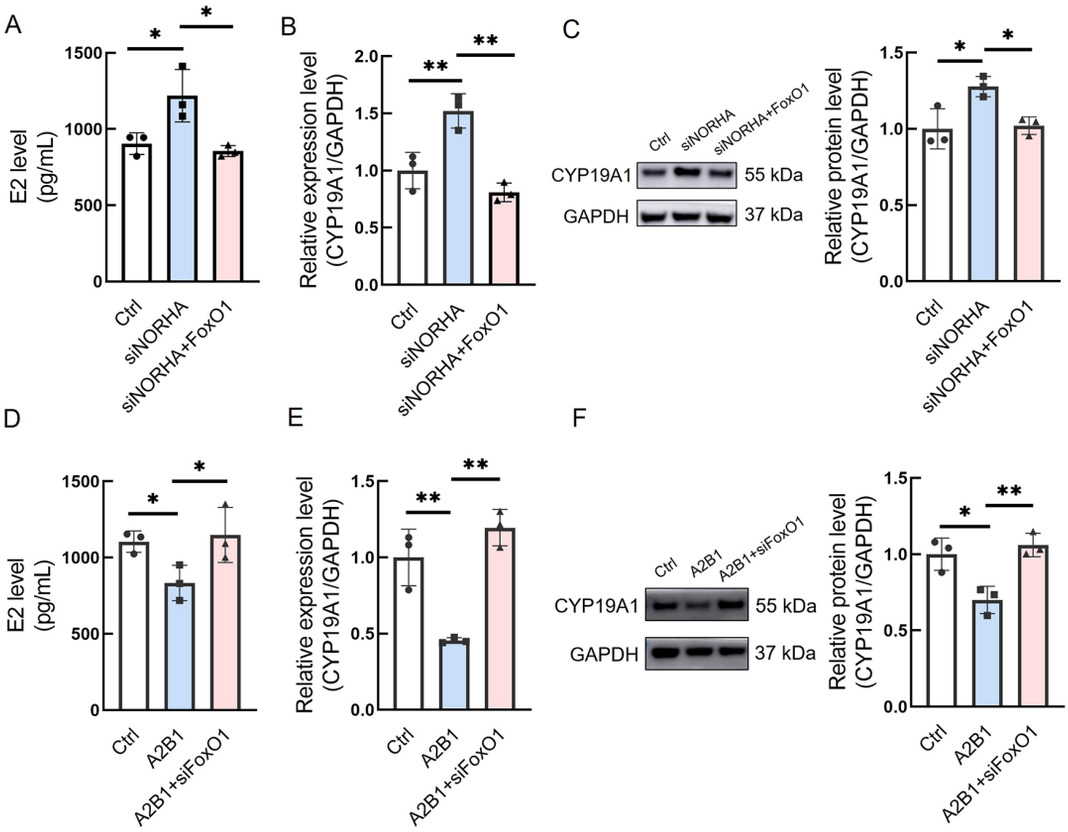

Figure 6 FoxO1 mediates HNRNPA2B1/NORHA axis regulation of E2 biosynthesis in sGCs

A–C: sGCs were co-transfected with NORHA-siRNA and pcDNA3.1-FoxO1, with E2 concentration in the culture medium (A) and CYP19A1 mRNA (B) and protein (C) levels then determined. D–F: sGCs were co-transfected with pcDNA3.1-HNRNPA2B1 and FoxO1-siRNA, with E2 concentration in the culture medium (D) and CYP19A1 mRNA (E) and protein (F) levels then determined. Values are mean±standard error. *: P<0.05; **: P<0.01.

A441, and A919 reporters (Figure 7G). Collectively, these findings demonstrate that METTL3 is involved in HNRNPA2B1 induction of NORHA m6A modification in sGCs via multiple m6A sites.

METTL3 regulates sGCs function via the HNRNPA2B1/NORHA axis

Based on evidence that the HNRNPA2B1/NORHA axis modulates E2 biosynthesis, the role of METTL3 in this process was further examined. Ectopic expression of METTL3 significantly reduced E2 concentrations in the culture medium (Figure 8A), indicating suppression of E2 biosynthesis in sGCs. Consistent with this, expression of CYP19A1 was markedly decreased in METTL3-overexpressing cells (Figure 8B, C). Furthermore, silencing HNRNPA2B1 reversed the declines in E2 concentration and CYP19A1 expression, while ectopic expressing NORHA restored the suppressive effects (Figure 8A–C), demonstrating that METTL3 exerts its regulatory function via the HNRNPA2B1/NORHA axis.

The impact of METTL3 on apoptosis was also assessed, given the pro-apoptotic role previously established for the HNRNPA2B1/NORHA pathway. As expected, ectopic expression of METTL3 significantly increased apoptosis in sGCs (Figure 8D). This pro-apoptotic effect was abolished by silencing HNRNPA2B1 and re-instated by co-expression of NORHA (Figure 8D; Supplementary Figure S11), indicating that METTL3 induces apoptosis through the same signaling cascade. Collectively, these findings demonstrate that METTL3 restrains E2 biosynthesis and induces apoptosis in sGCs via the HNRNPA2B1/NORHA axis. Notably, our results identified an m6A modification-related signaling pathway, METTL3/HNRNPA2B1/NORHA/CYP19A1, that coordinates key aspects of sGC function (Supplementary Figure S12).

DISCUSSION

LncRNAs, defined as transcripts longer than 200 nucleotides that lack the ability to encode functional proteins, exhibit limited sequence conservation across species, especially in comparison to mRNAs (Huang et al., 2024; Morales-Vicente et al., 2024). This evolutionary divergence restricts the utility of annotated lncRNAs from humans and model animals for cross-species extrapolation, particularly in the context of livestock genomics. Consequently, both the identification and functional characterization of lncRNAs in farm animals remain challenging, and the landscape of RNA modifications governing lncRNA stability and function in these species is largely unexplored. In the present study, m6A methylation was shown to regulate the stability of NORHA, an intergenic lncRNA, in sGCs. To the best of our knowledge, NORHA represents only the second identified lncRNA, after EN_42575, demonstrated to be regulated by m6A in pigs. EN_42575, the most strongly down-regulated lncRNA in CPB2 toxin-exposed intestinal porcine epithelial cells (IPEC-J2), is stabilized by METTL3 through an m6A-dependent mechanism and governs critical cellular processes, including proliferation and oxidative stress responses (Yang et al., 2023a). Collectively, our findings identified NORHA as an m6A-regulated lncRNA in sGCs, providing new mechanistic insights into post-transcriptional lncRNA regulation in swine and

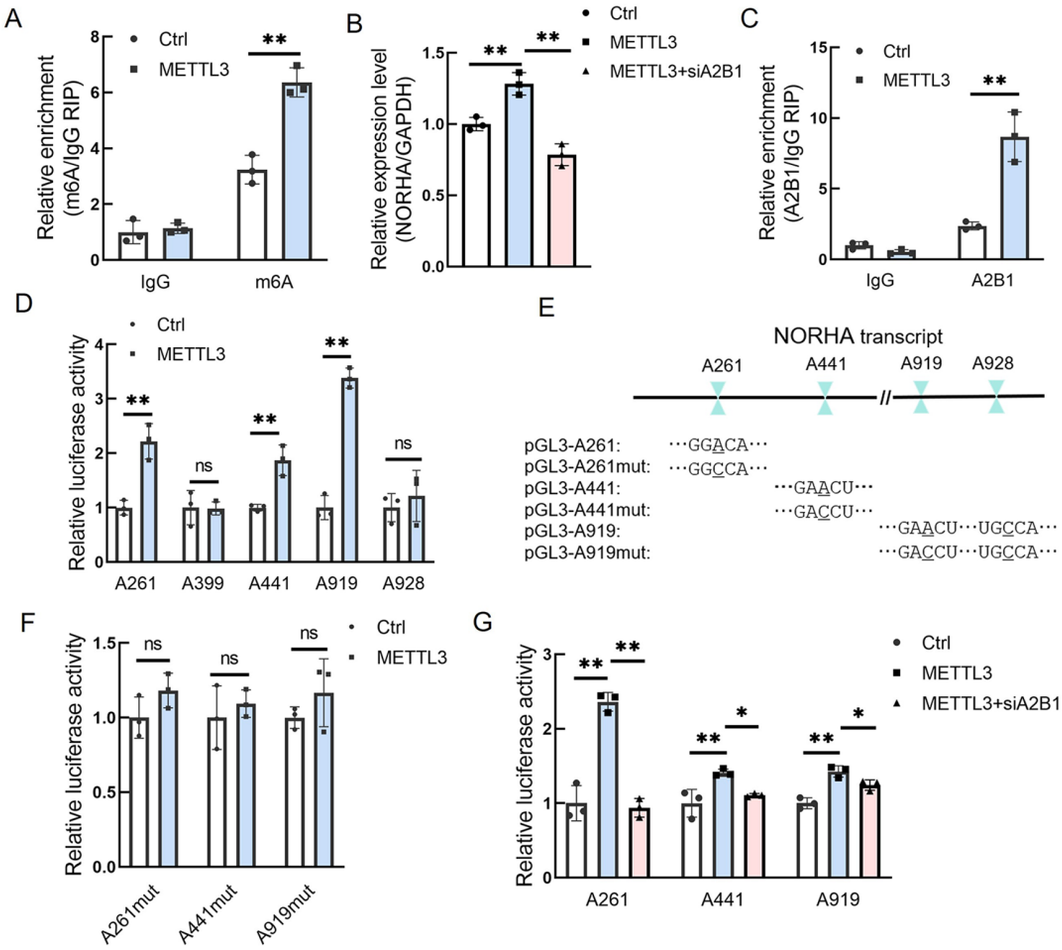

Figure 7 METTL3 is involved in HNRNPA2B1 induction of NORHA m6A modification in sGCs

A: sGCs were transfected with pcDNA3.1-METTL3, with m6A-containing NORHA RNAs then determined. B: sGCs were co-transfected with pcDNA3.1-METTL3 and HNRNPA2B1-siRNA, with NORHA expression then determined. C: sGCs were transfected with pcDNA3.1-METTL3, with HNRNPA2B1-interacting NORHA RNAs then determined. D: sGCs were co-transfected with pcDNA3.1-METTL3 and reporter vectors of NORHA, with luciferase activity then determined. E, F: Reporter vectors of NORHA with mutant-type m6A sites were constructed (E) and co-transfected with pcDNA3.1-METTL3 into sGCs, with luciferase activity then determined (F). G: sGCs were co-transfected with reporter vectors of NORHA, pcDNA3.1-METTL3, and HNRNPA2B1-siRNA, with luciferase activity then determined. Values are mean±standard error. *: P<0.05; **: P<0.01. ns: Not significant.

reinforcing the role of NORHA as a functional determinant of fertility-related processes in sGCs.

Mechanistically, HNRNPA2B1 maintains NORHA stability in sGCs by promoting m6A modification of multiple sites. As a multifunctional m6A reader, HNRNPA2B1 recognizes various target RNAs, including mRNAs, miRNAs, circRNAs, and lncRNAs (Alarcón et al., 2015; Hu et al., 2023; Vaid et al., 2024; Wang et al., 2019). In immune signaling, HNRNPA2B1 enhances m6A methylation on key mRNAs, such as *CGAS*, *STING*, and *IFI16*, thereby initiating innate immune programs against DNA viruses (Wang et al., 2019). In miRNA biogenesis, HNRNPA2B1 contributes to m6A modification of various transcripts, including pri-miRNAs, pre-miRNAs, and mature miRNAs via m6A-dependent interactions (Alarcón et al., 2015; Garbo et al., 2024). For circRNAs, recent evidence suggests that HNRNPA2B1 recognizes and interacts with m6A-modified circCCAR1 and mediates its sorting into exosomes in hepatocellular carcinoma (Hu et al., 2023). An increasing number of lncRNAs have also been identified as HNRNPA2B1 targets regulated through m6A modification (Vaid et al., 2024; Wang et al., 2024). Conversely, some lncRNAs have been implicated in modulating the stability of HNRNPA2B1 itself (Jin et al., 2024; Wen et al., 2024), underscoring a complex bidirectional regulatory relationship. Mounting evidence has also suggested that HNRNPA2B1 contributes to a wide range of cellular functions, including stemness maintenance, apoptotic signaling, and immune defense, by regulating the m6A epitranscriptome of key transcripts (Hu et al., 2023; Jin et al., 2024; Vaid et al., 2024; Wang et al., 2019). For instance, in breast cancer stem cells, HNRNPA2B1 has been shown to enhance nucleocytoplasmic trafficking of stemness maintenance-related mRNAs such as FGFR1, thereby facilitating cell self-renewal (Jin et al., 2024). However, most investigations into the role of HNRNPA2B1 in regulating cell function via m6A modification have predominantly focused on pathological contexts, especially cancer cells, with limited evidence from physiologically normal tissues and cells (Kwon et al., 2019). In this study, HNRNPA2B1 was associated with follicular atresia in sows, where it restrained E2 synthesis and induced apoptosis in sGCs by facilitating m6A modification of the lncRNA NORHA. These findings identify HNRNPA2B1 as an essential

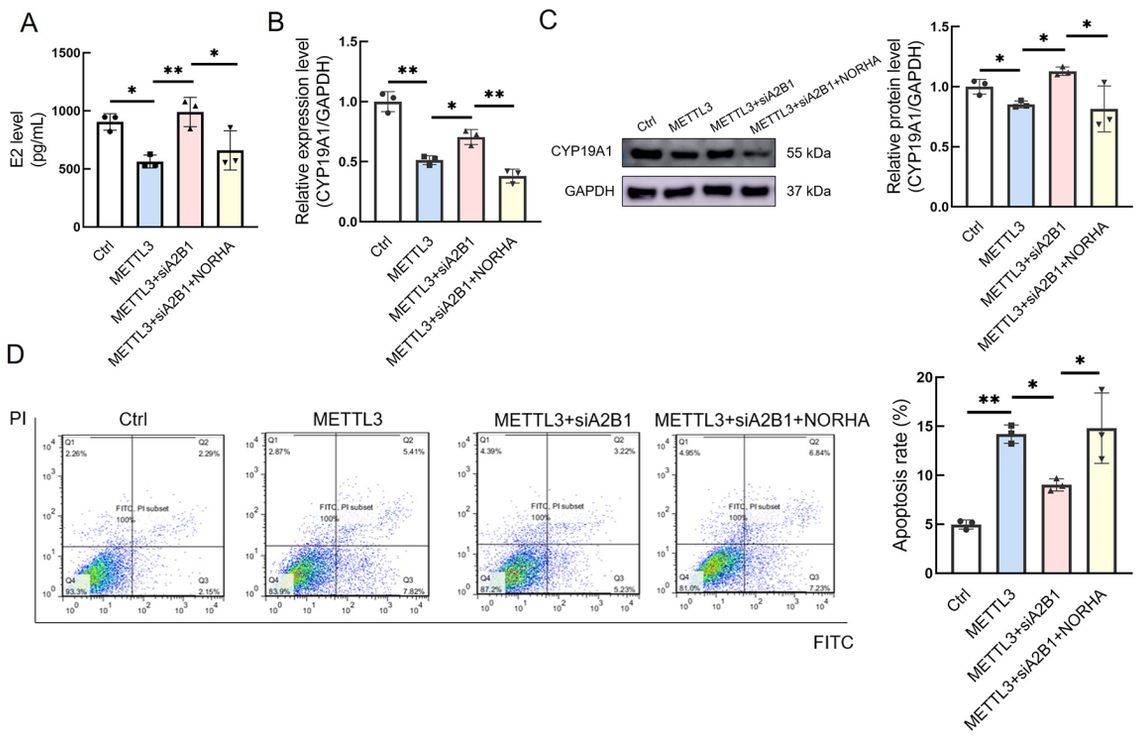

Figure 8 METTL3 controls sGC function via the HNRNPA2B1/NORHA axis

A–D: sGCs were co-transfected with pcDNA3.1-METTL3, HNRNPA2B1-siRNA, and pcDNA3.1-NORHA, with E2 concentration in the culture medium (A), CYP19A1 mRNA (B) and protein (C) levels, and apoptosis rate (D) then determined. Values are mean±standard error. *: P<0.05; **: P<0.01.

contributor to sGC function under normal physiological conditions and highlight its relevance as a potential molecular target for improving reproductive outcomes in sows.

NORHA has been strongly implicated in sow follicular atresia by promoting apoptosis in sGCs (Yao et al., 2021). Mechanistically, NORHA functions as a competing endogenous RNA by sequestering miRNAs that either suppress pro-apoptotic genes (FoxO1, SMAD7)—such as the miR-183 cluster and miR-423 —or enhance anti-apoptotic genes (TGFBR2, SMAD3)—such as miR-187 and miR-184 (Li et al., 2023; Shan et al., 2024; Yang et al., 2023b; Yao et al, 2021). Recent studies have also suggested that NORHA restrains NORFA, a functional lncRNA that reduces sGCs apoptosis (Du et al., 2021; Yang et al., 2023b). Interestingly, many downstream targets of NORHA are directly involved in E2 biosynthesis, a central function of GCs. For instance, miR-184 and NORFA have been reported to induce E2 production in sGCs (Du et al., 2021; Shi et al., 2022), while miR-96 (a component of the miR-183 cluster) and miR-423 regulate E2 biosynthesis in human GCs (Liu et al., 2023; Xie et al., 2020). Several of these targets, including TGFBR2, SMAD3, and SMAD7, are core members of the TGF-β signaling pathway, which is closely associated with E2 biosynthesis in GCs across species, including pigs, humans, and rodents (Cheng et al., 2021; Li et al., 2018; Yao et al., 2010). Despite these associations, the direct role of NORHA in E2 biosynthesis remained unresolved. The present study revealed that NORHA restrained E2 synthesis in sGCs by up-regulating FoxO1, a transcriptional repressor that inhibits CYP19A1 expression. These findings not only uncover a previously unrecognized function of NORHA in steroidogenesis, but also provide potential molecular targets for reproductive regulation in sow production.

As an important m6A reader, HNRNPA2B1 exhibits a strong functional association with METTL3, a central component of the m6A methyltransferase complex (Alarcón et al., 2015; Sun et al., 2023b; Vaid et al., 2024). Both proteins participate in overlapping regulatory processes within tissues and cells. In breast cancer, for instance, HNRNPA2B1 governs alternative splicing of exons in a manner analogous to METTL3 (Alarcón et al., 2015). Furthermore, knockout of either HNRNPA2B1 or METTL3 impairs miRNA biogenesis, and HNRNPA2B1 has been shown to facilitate miRNA processing by recognizing METTL3/m6A-dependent pri-miRNAs (Alarcón et al., 2015; Sun et al., 2023a). Consistently, most HNRNPA2B1-bound targets exhibit METTL3-dependent m6A methylation, and both proteins exert similar directional effects on their shared target RNAs (Supplementary Table S10). In this study, METTL3, like HNRNPA2B1, was shown to inhibit E2 biosynthesis and facilitate apoptosis in sGCs by enhancing the expression of NORHA and activating the NORHA/FoxO1/CYP19A1 pathway in an m6A-dependent manner. These findings reinforce the view that HNRNPA2B1 and METTL3 are closely related across multiple levels, including shared targets and biological outcomes.

In conclusion, this study identified NORHA as a novel m6A-regulated target of HNRNPA2B1 in sGCs and established HNRNPA2B1 as an essential regulator of sGC function, including E2 synthesis and apoptosis, via the novel NORHA/FoxO1/CYP19A1 pathway (Supplementary Figure S12). Furthermore, our findings demonstrated that METTL3 modulates the expression and function of this pathway through upstream control of HNRNPA2B1. Collectively, these findings provide the first evidence of m6A-dependent regulation of NORHA and provide potential molecular targets for the control of female reproductive function.

SUPPLEMENTARY DATA

Supplementary data to this article can be found online.

COMPETING INTERESTS

The authors declare that they have no competing interests.

AUTHORS' CONTRIBUTIONS

C.X.Z. and Q.F.L. completed experimental design and article writing. C.X.Z. and S.Q.W. conducted experiments and collected data. C.X.Z., J.Y.Z., and X.D. analyzed the data. All authors read and approved the final version of the manuscript.

REFERENCES

Alarcón CR, Goodarzi H, Lee H, et al. 2015. HNRNPA2B1 is a mediator of m^{6}A-dependent nuclear RNA processing events. *Cell*, **162**(6): 1299–1308.

Cai YT, Zhou JW, Xu AB, et al. 2024. N6-methyladenosine triggers renal fibrosis *via* enhancing translation and stability of *ZEB2* mRNA. *Journal of Biological Chemistry*, **300**(9): 107598.

Chen BX, Deng YR, Hong YT, et al. 2024. Metabolic recoding of NSUN2-mediated m^{5}C modification promotes the progression of colorectal cancer via the NSUN2/YBX1/m^{5}C-ENO1 positive feedback loop. *Advanced Science*, **11**(28): 2309840.

Cheng JC, Fang LL, Yan Y, et al. 2021. TGF-β1 stimulates aromatase expression and estradiol production through SMAD2 and ERK1/2 signaling pathways in human granulosa-lutein cells. *Journal of Cellular Physiology*, **236**(9): 6619–6629.

Du X, Li QQ, Yang L, et al. 2021. Transcriptomic data analyses reveal that sow fertility-related lincRNA *NORFA* is essential for the normal states and functions of granulosa cells. *Frontiers in Cell and Developmental Biology*, **9**: 610553.

Garbo S, D'Andrea D, Colantoni A, et al. 2024. m6A modification inhibits miRNAs' intracellular function, favoring their extracellular export for intercellular communication. *Cell Reports*, **43**(6): 114369.

Hu ZQ, Chen G, Zhao YP, et al. 2023. Exosome-derived circCCAR1 promotes CD8 + T-cell dysfunction and anti-PD1 resistance in hepatocellular carcinoma. *Molecular Cancer*, **22**(1): 55.

Huang WZ, Xiong TL, Zhao YT, et al. 2024. Computational prediction and experimental validation identify functionally conserved lncRNAs from zebrafish to human. *Nature Genetics*, **56**(1): 124–135.

Jin T, Yang LP, Chang C, et al. 2024. HnRNPA2B1 ISGylation regulates m6A-tagged mRNA selective export via ALYREF/NXF1 complex to foster breast cancer development. *Advanced Science*, **11**(24): 2307639.

Kwon J, Jo YJ, Namgoong S, et al. 2019. Functional roles of hnRNPA2/B1 regulated by METTL3 in mammalian embryonic development. *Scientific Reports*, **9**(1): 8640.

Li QQ, Du X, Pan ZX, et al. 2018. The transcription factor SMAD4 and miR-10b contribute to E2 release and cell apoptosis in ovarian granulosa cells by targeting CYP19A1. *Molecular and Cellular Endocrinology*, **476**: 84–95.

Li YQ, Zhang ZF, Wang SQ, et al. 2023. miR-423 sponged by lncRNA *NORHA* inhibits granulosa cell apoptosis. *Journal of Animal Science and Biotechnology*, **14**(1): 154.

Liu YJ, Zhang SS, Chen L, et al. 2023. The molecular mechanism of miR-96-5p in the pathogenesis and treatment of polycystic ovary syndrome. *Translational Research*, **256**: 1–13.

Morales-Vicente DA, Tahira AC, Woellner-Santos D, et al. 2024. The human developing cerebral cortex is characterized by an elevated de novo expression of long noncoding RNAs in excitatory neurons. *Molecular Biology and Evolution*, **41**(7): msae123.

Shan BS, Huo YA, Guo ZN, et al. 2024. miR-184, a downregulated ovary-elevated miRNA transcriptionally activated by SREBF2, exerts anti-apoptotic properties in ovarian granulosa cells through inducing *SMAD3* expression. *Cell Death & Disease*, **15**(12): 892.

Sheng WM, Wang MM, Li YQ, et al. 2024. Oxidative stress controls lncRNA-mediated sow granulosa cell functions in a FoxO1-dependent manner. *Journal of Animal Science and Biotechnology*, **15**(1): 171.

Shi SJ, Hu YM, Song XR, et al. 2022. Totipotency of miR-184 in porcine granulosa cells. *Molecular and Cellular Endocrinology*, **558**: 111765.

Sun HX, Li K, Liu C, et al. 2023a. Regulation and functions of non-m^{6}A mRNA modifications. *Nature Reviews Molecular Cell Biology*, **24**(10): 714–731.

Sun MH, Shen YH, Jia GZ, et al. 2023b. Activation of the HNRNPA2B1/*miR-93-5p*/FRMD6 axis facilitates prostate cancer progression in an m6A-dependent manner. *Journal of Cancer*, **14**(7): 1242–1256.

Vaid R, Thombare K, Mendez A, et al. 2024. METTL3 drives telomere targeting of TERRA lncRNA through m^{6}A-dependent R-loop formation: a therapeutic target for ALT-positive neuroblastoma. *Nucleic Acids Research*, **52**(5): 2648–2671.

Wang JY, Zhang JH, Liu H, et al. 2024. N6-methyladenosine reader hnRNPA2B1 recognizes and stabilizes NEAT1 to confer chemoresistance in gastric cancer. *Cancer Communications*, **44**(4): 469–490.

Wang L, Wen MY, Cao XT. 2019. Nuclear hnRNPA2B1 initiates and amplifies the innate immune response to DNA viruses. *Science*, **365**(6454): eaav0758.

Wang MM, Wang Y, Yang L, et al. 2023a. Nuclear lncRNA NORSF reduces E2 release in granulosa cells by sponging the endogenous small activating RNA miR-339. *BMC Biology*, **21**(1): 221.

Wang SQ, Li YQ, Zeng Q, et al. 2022. A mutation in endogenous saRNA miR-23a influences granulosa cells response to oxidative stress. *Antioxidants*, **11**(6): 1174.

Wang SQ, Wang Y, Chen YB, et al. 2023b. MEIS1 is a common transcription repressor of the miR-23a and NORHA axis in granulosa cells. *International Journal of Molecular Sciences*, **24**(4): 3589.

Wen Y, Yang XW, Li YF, et al. 2024. *DRAIC* mediates hnRNPA2B1 stability and m^{6}A-modified *IGF1R* instability to inhibit tumor progression. *Oncogene*, **43**(29): 2266–2278.

Wiener D, Schwartz S. 2021. The epitranscriptome beyond m^{6}A. *Nature Reviews Genetics*, **22**(2): 119–131.

Xie S, Zhang Q, Zhao J, et al. 2020. MiR-423-5p may regulate ovarian response to ovulation induction via CSF1. *Reproductive Biology and Endocrinology*, **18**(1): 26.

Yang JJ, Yang QL, Huang XY, et al. 2023a. METTL3-Mediated LncRNA *EN_42575* m6A Modification Alleviates CPB2 Toxin-Induced Damage in IPEC-J2 Cells. *International Journal of Molecular Sciences*, **24**(6): 5725.

Yang L, Du X, Wang SQ, et al. 2023b. A regulatory network controlling ovarian granulosa cell death. *Cell Death Discovery*, **9**(1): 70.

Yang L, Ying JM, Tao Q, et al. 2024a. RNA N^6-methyladenosine modifications in urological cancers: from mechanism to application. *Nature Reviews Urology*, **21**(8): 460–476.

Yang WL, Zhao YL, Yang YG. 2024b. Dynamic RNA methylation modifications and their regulatory role in mammalian development and diseases. *Science China Life Sciences*, **67**(10): 2084–2104.

Yao GD, Yin MM, Lian J, et al. 2010. MicroRNA-224 is involved in transforming growth factor-β-mediated mouse granulosa cell proliferation and granulosa cell function by targeting Smad4. *Molecular Endocrinology*, **24**(3): 540–551.

Yao W, Pan ZX, Du X, et al. 2021. NORHA, a novel follicular atresia-related lncRNA, promotes porcine granulosa cell apoptosis via the miR-183-96-182 cluster and FoxO1 axis. *Journal of Animal Science and Biotechnology*, **12**(1): 103.

Yu Y, Yang YL, Chen XY, et al. 2024. *Helicobacter pylori*-enhanced hnRNPA2B1 coordinates with PABPC1 to promote non-m^{6}A translation and gastric cancer progression. *Advanced Science*, **11**(30): 2309712.

Zaccara S, Ries RJ, Jaffrey SR. 2019. Reading, writing and erasing mRNA methylation. *Nature Reviews Molecular Cell Biology*, **20**(10): 608–624.

Zhao ZC, Qing Y, Dong L, et al. 2023. QKI shuttles internal m^{7}G-modified transcripts into stress granules and modulates mRNA metabolism. *Cell*, **186**(15): 3208–3226. e27.